Indian Journal of Geo Marine Sciences
Vol. 53 (04), April 2024, pp. 181-194
DOI: 10.56042/ijms.v53i04.10580

Design and performance assessment of a hydrographic unmanned surface vessel for enhanced autonomous bathymetry operations in shallow water areas

M A Norazaruddin[a,b], Z Z Abidin*[,a,b] & T A T Anuar[a,b]

[a]Department of Mechatronics, Kulliyah of Enginnering, International Islamic University, Malaysia, Kuala Lumpur – 53100, Malaysia

[b]Centre for Unmanned Technologies (CUTe), International Islamic University Malaysia, Kuala Lumpur – 53100, Malaysia

*[Email: zzulkifli@iium.edu.my]

Received 21 January 2024; revised 19 April 2024

This paper details the development and performance evaluation of an Unmanned Surface Vessel (USV) designed for enhanced autonomous bathymetry in shallow water areas. Through significant technological enhancements, including the integration of a CXSense controller, M1G2 GNSS receiver, KVH C100 magnetic compass, and SBG System INS, the USV demonstrated exceptional operational capabilities. Performance metrics revealed a cross-track error of 0.92 to 2.39 meters, surpassing the International Hydrographic Organization's Category 2 standards. The study outlines the comprehensive upgrades undertaken on the USV's propulsion, GNSS positioning, course control, and data transmission systems, which collectively facilitated robust automated operations. The successful deployment of low-cost multi-GNSS receivers illustrates a shift toward more economical hydrographic survey methods, challenging the need for expensive professional-grade equipment. The findings underscore the potential of USVs in revolutionising hydrographic surveying, offering substantial improvements in cost-efficiency, operational flexibility, and data accuracy, thereby enhancing marine research and commercial maritime operations.

[**Keywords**: Autonomous bathymetry, Autonomous navigation, Hydrographic surveying, Maritime technology, Unmanned Surface Vessel]

Introduction

Hydrography, the science of mapping the Earth's water-covered surfaces, is fundamental for enhancing navigation through the precise measurement of depths and the production of accurate bathymetric charts. This precision is achieved through selecting advanced technical equipment, meticulous planning, exact execution of measurements, and thorough data processing[1–3]. Additionally, the integration of new datasets from opportunistic and research expeditions has significantly improved the quality and coverage of bathymetric charts[4,5].

The evolution of bathymetric surveys has been notably enhanced by adopting Multibeam Echosounders (MBES) combined with Global Navigation Satellite Systems (GNSS). This technology, ranging from marine Differential Global Positioning System (DGPS) providing 1 – 2 m accuracy to geodetic network solutions offering 2 – 5 cm accuracy, has dramatically improved the quality of bathymetric data[1,6]. Integrating MBES and GNSS allows for detailed and accurate mapping of underwater terrains, which is crucial for safe navigation, marine research, and environmental monitoring.

Despite the well-established usage of GNSS, IMU, hydrographic tools, and autopilot PID controllers in unmanned boats, there remains a significant challenge in achieving high-precision navigation and data acquisition in shallow water areas. This study aims to address this challenge by integrating advanced control systems and sensor technologies to enhance the operational efficiency, accuracy, and reliability of hydrographic USVs in aquatic environments.

In the 21st century, advancements in autonomous vessel technology have significantly expanded the use of unmanned vessels in hydrographic surveys. These vessels, featuring various hull designs and propulsion systems, are particularly suited for operations in shallow waters[1]. The rise of small unmanned vessels has revolutionised hydrography, enabling access to water bodies that were previously challenging or inaccessible. This shift towards Unmanned Surface Vessels (USVs) represents a significant technological leap, promising further enhancements in the accuracy and efficiency of hydrographic surveys[7].

A comprehensive review of path-planning techniques for Autonomous Marine Vehicles (AMVs) highlights the integration of both terrestrial and non-

terrestrial networks, essential for achieving full-dimensional wireless coverage in marine environments. Advanced algorithms and machine learning techniques are emphasised to overcome challenges such as sensor failures, inaccurate state estimations, and complex ocean dynamics[8]. These innovations significantly improve the efficiency and reliability of maritime data collection.

Materials and Methods

Platform hardware description

The research project began with a technological overhaul of a hydrographic USV. Initially, this trimaran—a compact vessel previously operated solely via Radio Control (RC)—lacked autonomous navigation capabilities. Constructed by Radio Control Models and Toys in Heraklion, Greece, the USV featured a single main hull flanked by two fibreglass buoyant bodies linked by aluminium rods, enhancing stability under environmental and mechanical stresses (depicted in Fig. 1). The hydrographic USV has a length of 1.33 meters, a width of 1.29 meters, and a weight of approximately 20 kgs. The propulsion system consists of two high-power Brushless DC (BLDC) motors, each providing a thrust of 50 N, equipped with 30A Electronic Speed Controllers (ESCs). These thrusters are allocated in a dual configuration to enable efficient and precise manoeuvring capabilities. The primary goal of these upgrades was to allow the USV to conduct automated hydrographic surveys autonomously, following pre-defined sounding profiles without operator intervention. Additionally, the upgrades aimed to extend the vessel's operational range and duration, increase the reliability of its components and overall system, and enhance its navigational capabilities.

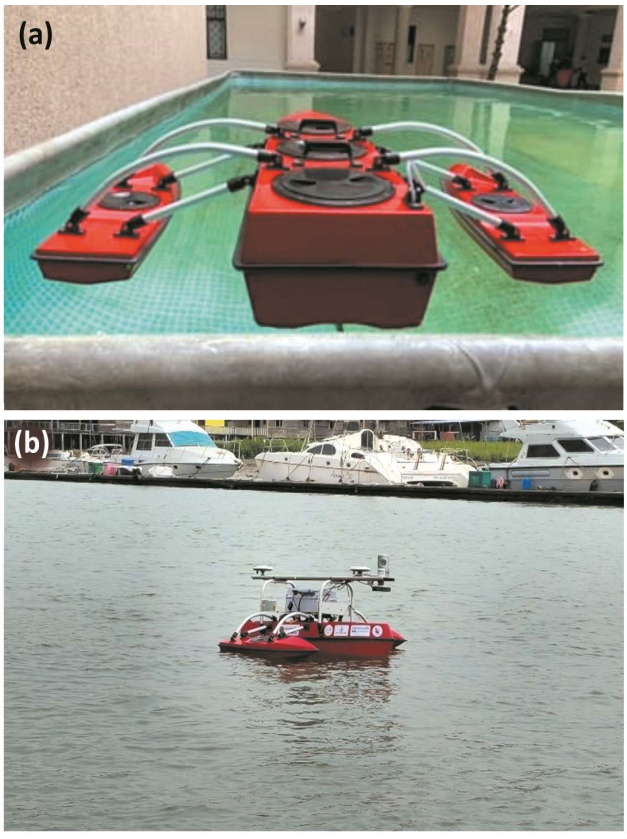

Fig. 1 — Comparative visualisation of the Unmanned Surface Vessel (USV): (a) Prior to; and (b) Following the upgrades

The selection of sensors was based on their accuracy, reliability, and suitability for hydrographic surveying in shallow waters. The M1G2 GNSS receiver was chosen for its high precision in positioning; while the KVH C100 Compass Engine and SBG System INS were selected for their superior performance in heading and inertial measurements. The measurement plan involved conducting surveys along predefined routes, with data acquisition systems configured to log positional and depth data continuously.

Central to the USV's modernisation was the installation of the CXSense control box, which introduced advanced autopilot functionalities and AI-driven obstacle avoidance and detection systems, allowing for intelligent autonomous navigation. The traditional RC microwave transmission system was replaced by a wireless radio access point (Bullet M2 2.4GHz HP), effectively tripling the vessel's operational range. Navigation accuracy was augmented with a high-quality heading GNSS receiver (eSurvey M1G2) and a KVH C100 compass engine, ensuring precise autopilot control. The propulsion system was upgraded to include two high-power Brushless DC (BLDC) motors, each providing 50 N of thrust and equipped with 30A Electronic Speed Controllers (ESCs). To boost operational endurance, the vessel was fitted with dual Lithium Polymer (LiPo) batteries, each with a 40 Ah capacity (illustrated in Fig. 2 with a schematic diagram of the electrical connections).

While the vessel’s drive, control, telemetric, and positioning systems underwent substantial modernisation, the hydrographic system was retained in its original configuration. It included a geodetic GNSS receiver and a Single Beam Echo Sounder (SBES), the SS510 EchoRange™, which already met

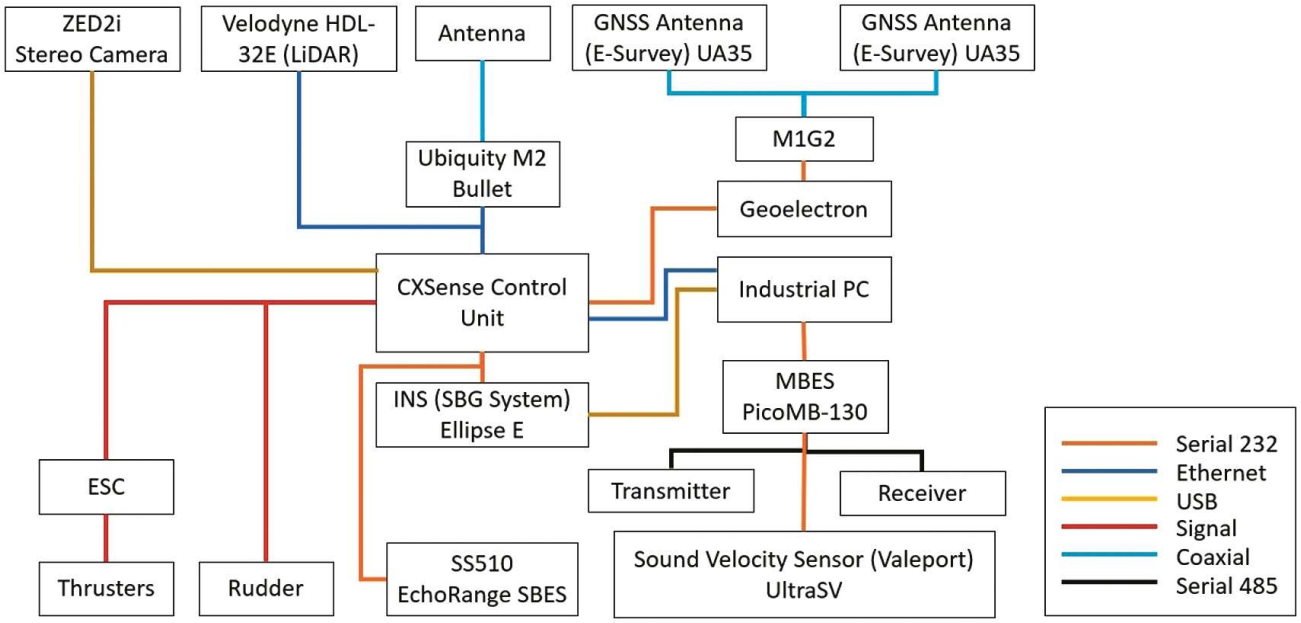

Fig. 2 — Schematic diagram of the main components integrated into the Unmanned Surface Vessel (USV)

Table 1 — Technical upgrades and operational enhancements of the hydrographic USV

Component	Original specification	New specification	Category
Control system	Direct RC	Manual, Semi-Autonomous, Autonomous	
Autopilot system	None	eSurvey M1G2, KVH C100, INS SBG system	
Obstacle avoidance	None	Velodyne HDL-32E LiDAR, ZED 2i camera	
Communications	RC transmission	Bullet M2 2.4GHz HP	
Telemetry monitoring	None	Integrated with control system	
Operational range	30 m (49 MHz)	1 km (2.4GHz)	
Propulsion	BLDCs	BLDCs (no change)	
Battery system	18 Ah LiPo	40 Ah LiPo	
Time of operation	3 – 4 h	6 – 8 h	
Hydrographic system	None	SBES, Velodyne HDL-32E LiDAR	
Vehicle weight	10 kg	20 kg	
Cooling and ESC	Forced, water-cooling	Forced, water-cooling	
Ingress protection	IP44	IP56	

Navigation Operational

the stringent standards of the International Hydrographic Organization (IHO). Table 1 details the comprehensive scope of these enhancements, listing the basic technical characteristics and operational properties targeted for modernisation. This table showcases the extent and focus of the improvements made to the USV.

Data acquisition system

The integration of USVs has significantly advanced the field of hydrographic surveying. These vessels combine sophisticated data acquisition systems with robust software solutions designed to automate the collection and analysis of aquatic environmental data. This automation supports navigational activities in both inland and sea water environments. Hydrographic USVs can be operated through direct radio control for manual tasks or via advanced autopilot systems for automated navigation. The automated mode enables the vessel to execute pre-planned routes with precision. These routes are meticulously designed using high-resolution orthophoto maps from platforms like Google Maps, providing detailed groundwork for comprehensive survey planning and execution.

As depicted in Figure 3, the telemetry system of the USV bridges the onshore control units with the vessel's onboard computational mechanisms.

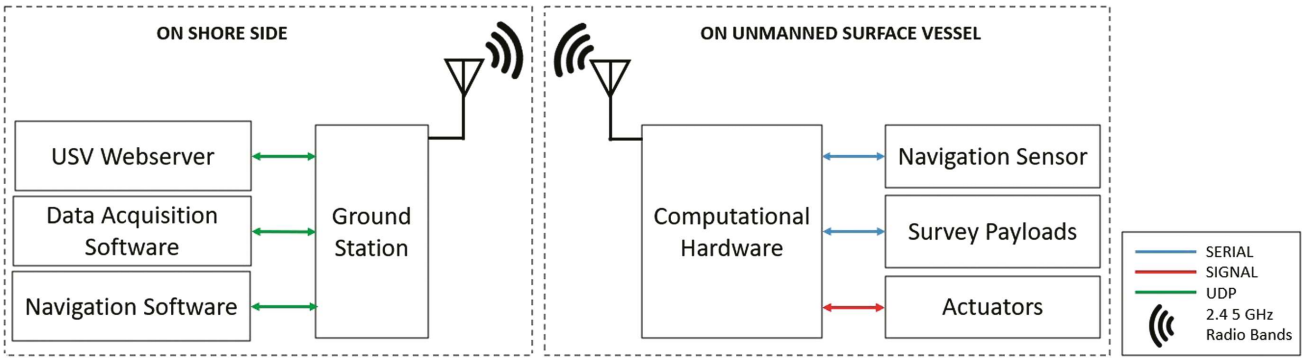

Fig. 3 — Block diagram of the telemetry system for the Unmanned Surface Vessel (USV)

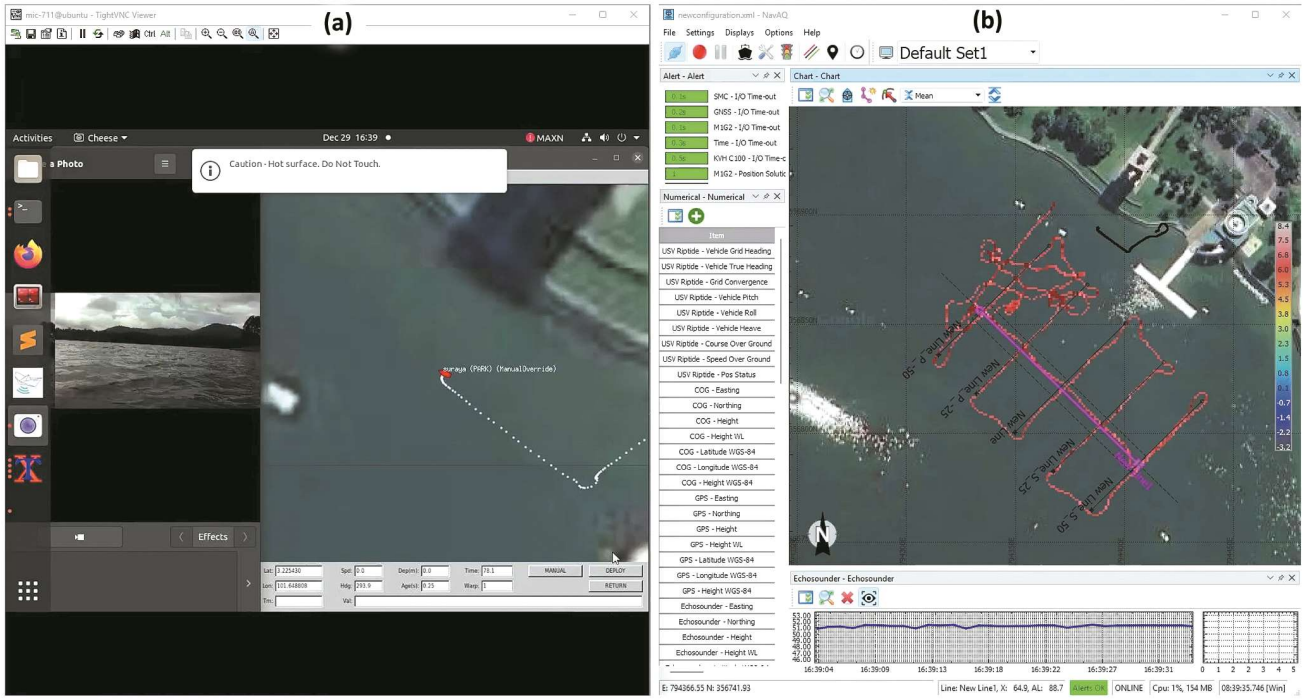

Fig. 4 — Software applications utilised for autonomous bathymetry survey operations: (a) MOOS-IvP; and (b) NavAq

Onshore, a web server interfaces with data acquisition and navigation software, enabling remote monitoring and dynamic route planning. Communication with the USV is maintained via a ground station using 2.4 GHz radio bands, which send navigational commands to the USV's computational hardware. This hardware processes data from navigation sensors and orchestrates the operation of survey payloads. Actuators on the USV carry out mechanical movements based on these commands, utilising various communication protocols such as serial connections for critical control signals and UDP for swift, real-time data transmission. This setup optimises the balance between speed and reliability in data exchange and navigational control.

In terms of software, hydrographic USVs employ a range of specialised tools to enhance operational efficiency and data accuracy. These software platforms enable real-time tracking of the vessel's position and integrate GPS data with navigational commands. They can adjust routes instantaneously based on environmental feedback, crucial in dynamic conditions that may alter pre-set paths. Popular software solutions for maritime navigation encompass a range of options, from open-source platforms like OpenCPN, which is recognized for its adaptability and extensive user support, to specialized commercial systems such as Beamworx and QINSY, as illustrated in Figure 4. These systems offer robust functionalities tailored to the complex needs of hydrographic

surveys, including real-time data processing, multi-vessel control, and sophisticated mapping capabilities.

USV Guidance, Navigation and Control (GNC)

The modernised hydrographic USV features an intricately designed Guidance, Navigation, and Control (GNC) system that enhances operational efficiency and precision in autonomous navigation. The system's architecture is comprised of advanced technological integrations such as GNSS, INS SBG system, Velodyne HDL-32E LiDAR, and ZED 2i camera. These components collaboratively ensure precise pathfinding, obstacle avoidance, and adherence to pre-defined waypoints, enabling the USV to autonomously execute complex hydrographic surveys. The guidance system formulates navigation paths, the navigation tools confirm positional accuracy, and the control system dynamically adjusts the USV's propulsion to meet survey requirements, illustrating a sophisticated interplay between technology and operational demands.

High-level controller

The GNC system's modernisation is epitomised by the integration of the MOOS-IvP framework (Fig. 5). This framework, operating on a star topology with a publish-subscribe model, centralises communication through the MOOS Database (MOOSDB). Each application, running independently but collaborating via the MOOSDB, adjusts its communication frequency based on user settings. This system architecture ensures a flexible and scalable design. Within the MOOS-IvP framework, core applications such as pHelmIvP act as decision-making centres by assimilating sensor data to command navigation. pNodeReporter disseminates vessel states, while applications like pMarineViewer and resource monitors (uMemwatch and uProcessWatch) ensure real-time visualisation and system health monitoring.

The Extended MOOS-IvP Tree includes iPayloadParser and pCoordinate Converter, enhancing data interpretation and coordinate system conversions. The seamless interfacing of these software components with the USV's hardware allows navigational sensors to transmit data to the microcontroller, which then translates it into mechanical actions through actuators. The GNC system employs an embedded obstacle detection algorithm for initiating avoidance manoeuvres and a PID controller to refine thrust and rudder settings, maintaining the desired navigational course. This control loop is constantly monitored for task fulfilment, ensuring the USV's adherence to operational parameters and demonstrating the system's adaptability and precision in maritime autonomy. Table 2 presents the high-level navigation process.

Low-level controller

The low-level controller forms the execution layer of the USV's autonomous operations, interfacing directly with the vessel's physical components. The vessel's dynamics are modelled based on standard marine kinematic equations, encompassing positional coordinates (x, y, z) and orientation angles (roll, pitch, yaw). The kinematic model includes surge, sway, and heave motions, described by the relationships between

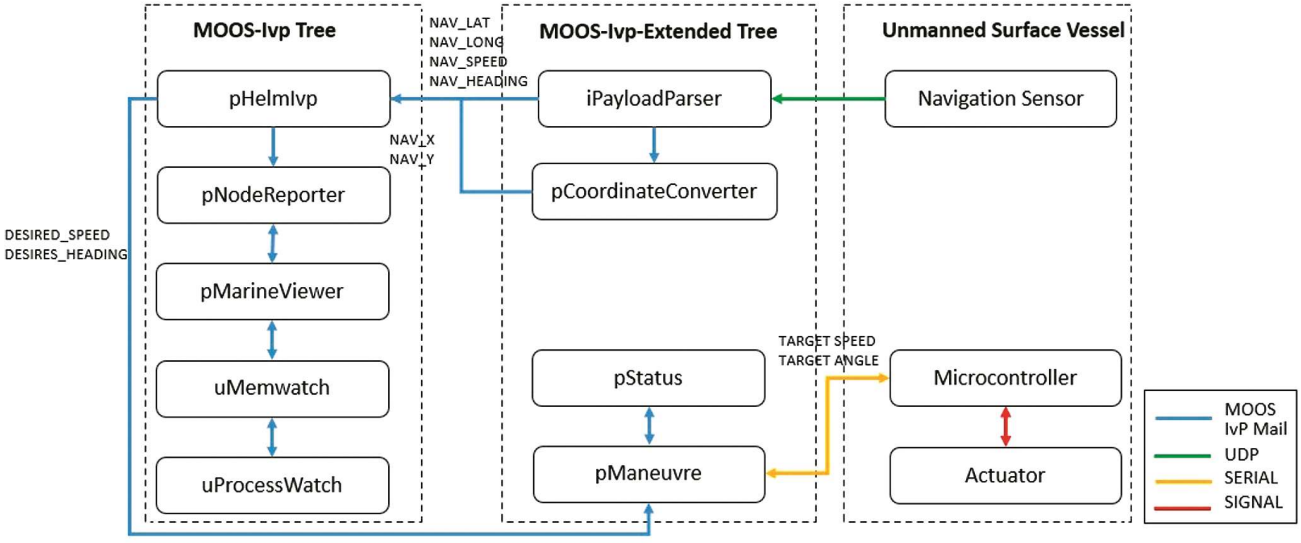

Fig. 5 — Software architecture of the Guidance, Navigation, and Control (GNC) system on an Unmanned Surface Vessel (USV)

Table 2 — USV navigation control process stages

Algorithm 1: High-level USV autonomous navigation
procedure Autonav_Control(Start)
initialize Nav_Data ← Parse_NMEA()
initialize Desired_Behavior ← Helm_IVP(Nav_Data)
while USV Operating **do**
Obs_Data ← Detect_Method()
obstacle_detected ← Detect_Obstacle(Obs_Data)
if obstacle_detected then
collision_risk ← Check_Collision(Obs_Data)
if collision_risk then
(V_d, θ_d) ← Avoidance_Behavior(Obs_Data) |
end if
else
(V_d, θ_d) ← Continue_Behavior(Desired_Behavior)
end if
(T_d, ϕ_d) ← PID_Control (V_d, θ_d)
Execute (Control_Actions (T_d, ϕ_d))
behavior_complete ←
Check_Behavior_Complete(Desired_Behavior)
if behavior_complete then
break
end if
end while
return *stop*
end procedure

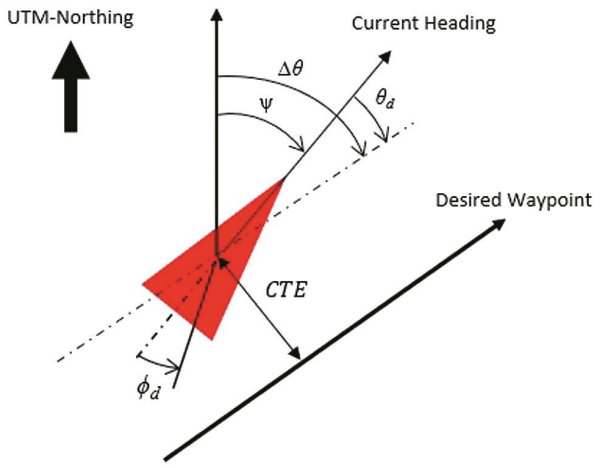

Fig. 6 — Line-following navigation diagram of the Unmanned Surface Vessel (USV) platform

these movements and the applied control inputs, such as thrust and rudder angles (Fig. 6).

The position of the USV in the global coordinate system is represented by (x, y, z), and its orientation by (φ, θ, ψ). These parameters are combined into a state vector $\vec{S} = [x, y, z, \phi, \theta, \psi]^T$. The kinematic equations describe how position and orientation change over time due to these velocities, as shown in Eq. (1). Similarly, the orientation angles (φ, θ, ψ) change based on the angular velocities and their respective trigonometric relationships, as shown in Eq. (2).

$$\begin{pmatrix} \dot{x} \\ \dot{y} \\ \dot{z} \end{pmatrix} = \begin{pmatrix} \cos\psi\cos\theta & -\sin\psi\cos\theta & \sin\theta \\ \sin\psi\cos\phi + \cos\psi\sin\theta\sin\phi & \cos\psi\cos\phi - \sin\psi\sin\theta\sin\phi & -\cos\theta\sin\phi \\ \sin\psi\sin\phi - \cos\psi\sin\theta\cos\phi & \cos\psi\sin\phi + \sin\psi\sin\theta\cos\phi & \cos\theta\cos\phi \end{pmatrix} \quad \ldots (1)$$

$$\begin{pmatrix} \dot{\phi} \\ \dot{\theta} \\ \dot{\psi} \end{pmatrix} = \begin{pmatrix} 1 & \sin\phi\tan\theta & \cos\phi\tan\theta \\ 0 & \cos\phi & -\sin\phi \\ 0 & \sin\phi/\cos\theta & \cos\phi/\cos\theta \end{pmatrix} \begin{pmatrix} p \\ q \\ r \end{pmatrix} \quad \ldots (2)$$

The control inputs for the USV are the thrust force (T) and the rudder angle (δ), which are applied to the dynamic equations to determine the resulting accelerations and velocities. The dynamic equations relate the forces and moments acting on the vessel to its accelerations in the surge, sway, and heave directions and its angular accelerations in roll, pitch, and yaw, as shown in Eq. (3).

$$\begin{pmatrix} \dot{u} \\ \dot{v} \\ \dot{w} \end{pmatrix} = \begin{pmatrix} rv - qw + g\sin\theta + \frac{X}{m} \\ pw - ru - g\cos\theta\sin\phi + \frac{Y}{m} \\ qu - pv - g\cos\theta\cos\phi + \frac{Z}{m} \end{pmatrix} \quad \ldots (3)$$

The autonomous design for the USV utilises the Nomoto model, a simplified linear model commonly used for ship manoeuvring. This model effectively captures the essential dynamics of the vessel's yaw motion in response to rudder inputs. The first-order Nomoto model is expressed in Eq. (4), where $\dot{\psi}$ represents the yaw rate, T is the time constant, K is the control gain, and δ is the rudder angle.

$$\dot{\psi} + T\dot{r} = K\delta \quad \ldots (4)$$

The parameters T T and K K are determined through system identification techniques, which involve analysing the USV's response to specific control inputs. These parameters are critical for accurate modelling of the USV's manoeuvring behaviour. By utilising the Nomoto model, the autopilot can effectively predict and adjust the vessel's heading, ensuring stable and precise navigation[2,3].

PID control applied to both heading and speed continuously adjusts the rudder angle and thrust based on calculated errors, which are derived from the differences between current and target values, as shown in Figure 7. This dynamic adjustment significantly enhances the USV's ability to follow a predetermined path with minimal deviation, optimising fuel consumption even in the presence of external disturbances such as currents and winds.

The design of the PID controller for the USV is crucial for maintaining accurate and stable navigation.

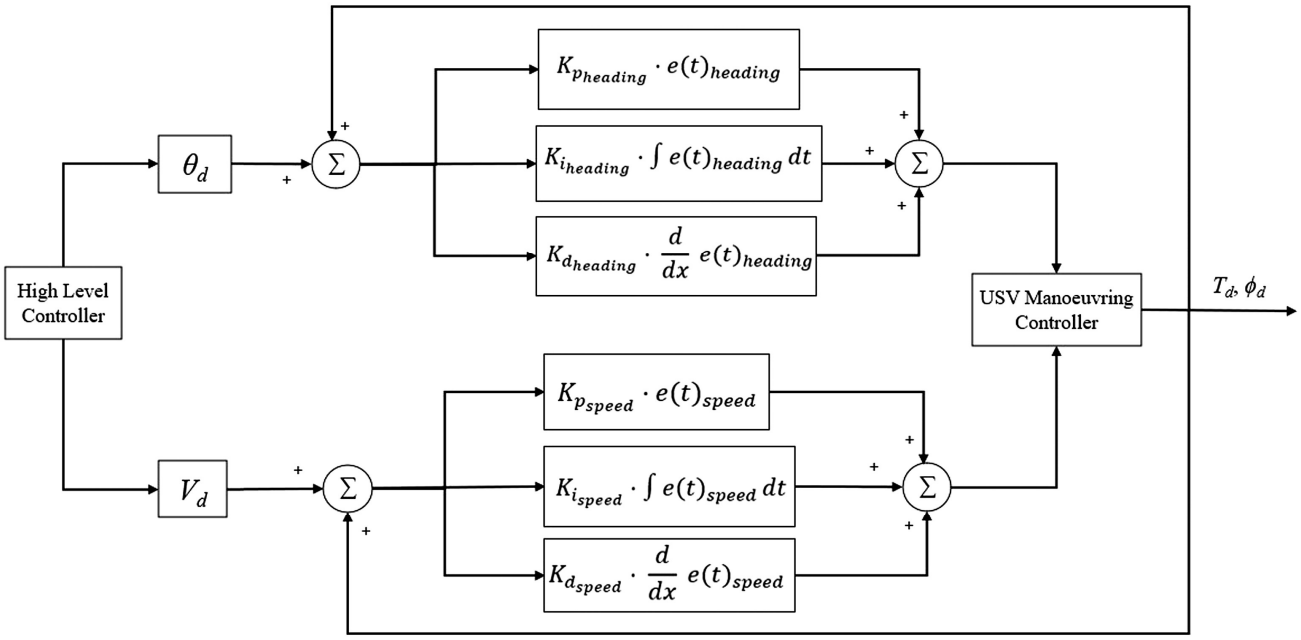

Fig. 7 — Autopilot PID block diagram for the Unmanned Surface Vessel (USV) navigation system

The PID controller adjusts the rudder angle and thrust based on the errors in heading and speed, continuously computing the difference between the desired and actual values of these parameters. The proportional term (K_p) produces an output value proportional to the current error value, the integral term (K_i) accounts for the accumulation of past errors, and the derivative term (K_d) considers the rate of change of the error, helping to reduce overshoot and settling time. The control laws for heading and speed are given in Eqs. (5) & (6), where θ_{error} and v_{error} are the differences between desired and actual values.

$$\delta = K_p\theta_{error} + K_i\int \theta_{error}dt + K_d \frac{d\theta_{error}}{dt} \quad \text{... (5)}$$

$$T = K_p v_{error} + K_i\int v_{error}dt + K_d \frac{dv_{error}}{dt} \quad \text{... (6)}$$

Tuning of the PID parameters (K_p, K_i, K_d) is critical for ensuring the USV to follow the desired trajectory with minimal deviation, even under external disturbances such as currents and winds. The PID control system dynamically adjusts the rudder angle and thrust, significantly enhancing the USV's ability to follow a predetermined path, optimising fuel consumption, and maintaining stability. This ensures precise manoeuvring and effective operation in hydrographic surveying missions. The control algorithm derived from the kinematic model links the parameters and states defined by the USV's kinematics, allowing for accurate and responsive control actions.

A control algorithm is crafted from the kinematic model, which is intrinsically linked to the parameters and states defined by the USV's kinematics, as shown in Table 3. The control logic is responsible for actuating the rudder and thrusters so that the vessel follows the desired trajectory as closely as possible, given its physical capabilities and environmental constraints.

Performance validation

The assessment of the modernised USV operational properties was conducted through experimental testing aimed at evaluating the accuracy of the USV's autonomous navigation along the pre-defined sounding profiles. The testing was performed under controlled conditions to minimise environmental impacts on data accuracy. Specifically, the experiments took place in windless weather, with the sea state at 0 on the Douglas scale, indicating no wind, waves or sea currents. The chosen waterbody for this study was a small lake in Tasik Metropolitan, providing a stable environment for precise measurements.

The modernised USV, outfitted with a survey-grade GNSS receiver, executed hydrographic surveys along pre-defined sounding profiles with varying configurations, including a waypoint grid of 100×100 m at 25 m intervals, and the inclusion of one crossline to broaden the survey's scope. The full

Table 3 — Low level control algorithm

Algorithm 2: Low-level dynamic control for USV

Inputs:

$x, y, \theta, V, x_{target}, y_{target}, V_{target}$

Constants and Parameters:

$\phi_{max}, T_{max}, T_{min}, \Delta\theta_{tol}, \Delta V_{tol}, S_{rudder}, S_{thurster}$

PID Constants:

$Kp_\theta, Ki_\theta, Kd_\theta,$

Kp_V, Ki_V, Kd_V

procedure:

Calculate_Heading_Error ()

$\theta_{err} \leftarrow atan2(y_{target} - y, x_{target} - x) - \theta$

Normalize θ_{err} *to* $[-\pi, \pi]$

Calculate_Speed_Error ()

$V_{err} \leftarrow V_{target} - V$

Calculate_Desired_Rudder_Angle ()

$\phi_d \leftarrow S_{rudder} * \theta_{err}$

Calculate_Desired_Thrust ()

if $|\theta_{err}| < \Delta\theta_{tol} \wedge |V_{err}| < \Delta V_{tol}$ ***then***

$T_d \leftarrow V$

else

$T_d \leftarrow S_{thurster} * V_{err}$

$T_d \leftarrow$ **CLAMP** (T_d, T_{min}, T_{max})

Calculate_PID_Control ()

$\int \boldsymbol{e_\theta} \leftarrow \int \boldsymbol{e_\theta} + \theta_{err}$

$\frac{\boldsymbol{d}}{\boldsymbol{dt}} \boldsymbol{e_\theta} \leftarrow \theta_{err} - e_{\theta,prev}$

$PID_\theta \leftarrow Kp\_heading * \theta_{err} + Ki_\theta * \int \boldsymbol{e_\theta} + Kd_\theta * \frac{\boldsymbol{d}}{\boldsymbol{dt}} \boldsymbol{e_\theta}$

$\int \boldsymbol{e_V} \leftarrow \int \boldsymbol{e_V} + V_{err}$

$\frac{\boldsymbol{d}}{\boldsymbol{dt}} \boldsymbol{e_V} \leftarrow V_{err} - e_{V,prev}$

$PID_V \leftarrow Kp_V * V_{err} + Ki_V * \int \boldsymbol{e_V} + Kp_V * \frac{\boldsymbol{d}}{\boldsymbol{dt}} \boldsymbol{e_V}$

Apply_PID_Controls ()

$\phi_d \leftarrow \phi_d + PID_\theta$

$\phi_d \leftarrow$ **CLAMP** $(\phi_d, -\phi_{max}, \phi_{max})$

$T_d \leftarrow T_d + PID_V$

$e_{\theta,prev} \leftarrow \theta_{err}$

$e_{V,prev} \leftarrow V_{err}$

output:

T_d, ϕ_d

end procedure

survey was completed in approximately 18 minutes, traversing 800 meters at a speed of 1 meter per second. The USV's motor battery supported up to 5 h of continuous operation, enabling six waypoint runs, while the system's battery sustained up to two days of operation, as illustrated in Figure 8.

The test routes for the hydrographic survey were planned using Beamworx Nav Aq geodetic software, with additional route details refined using satellite images from Google Earth. The coordinates of the route turning points were exported into *.kml files, recorded as geodetic coordinates referenced to the WGS84 ellipsoid. The planned USV routes were then converted to *.bhv files compatible with the MOOS-IvP framework, which operates the CXSense control box installed on the vessel.

During the navigation trials, the position coordinates recorded by the geodetic GNSS receiver—latitude and longitude—were continually logged. These coordinates were mapped with the designed survey line, projecting the geographic coordinates from the surface of the World Geodetic System 1984 (WGS84) ellipsoid.

Results

Navigation error analysis

The accuracy of the USVs navigation system in maintaining the set course along the predetermined waypoints is crucial for the success of maritime missions. This section evaluates the system's performance by analysing various types of navigation errors, such as cross-track errors, cumulative errors, and employs interpolation techniques to standardise the analysis of temporal data.

Cross-Track Error (CTE)

Cross-Track Error (CTE) is a key metric for assessing the USV's adherence to its intended course, calculated as the shortest perpendicular distance from the USV's navigational path to the designated waypoint path, as shown in Figure 8. This error is calculated for each navigation point using Eq. (3), where nav represents the current navigation coordinates, $wp1$ and $wp2$ are consecutive waypoints, and $d_{perpendicular}$ is the perpendicular distance from the navigation point to the line segment defined by $wp1$ and $wp2$. This calculation is iteratively performed for each navigation point against all waypoint segments, providing a detailed evaluation of navigation precision.

$$CTE = min_{\forall(wp1,wp2)} | d_{perpendicular}(nav, (wp1, wp2) | \quad \ldots (7)$$

Cumulative error

The cumulative error is computed to evaluate the overall navigational accuracy over the course of a voyage. This cumulative metric sums all individual cross-track errors, providing an aggregate measure of the deviation experienced during the journey as shown in Eq. 4. Each $CT\ Ei$ corresponds to the cross-track error calculated at the i-th navigation point. This aggregate error helps understand the total deviation from the planned path, highlighting the effectiveness of the navigation system and identifies any consistent error patterns.

$$Cumulative\ Error = \sum_{i=1}^{n} CT\ Ei \quad \ldots (8)$$

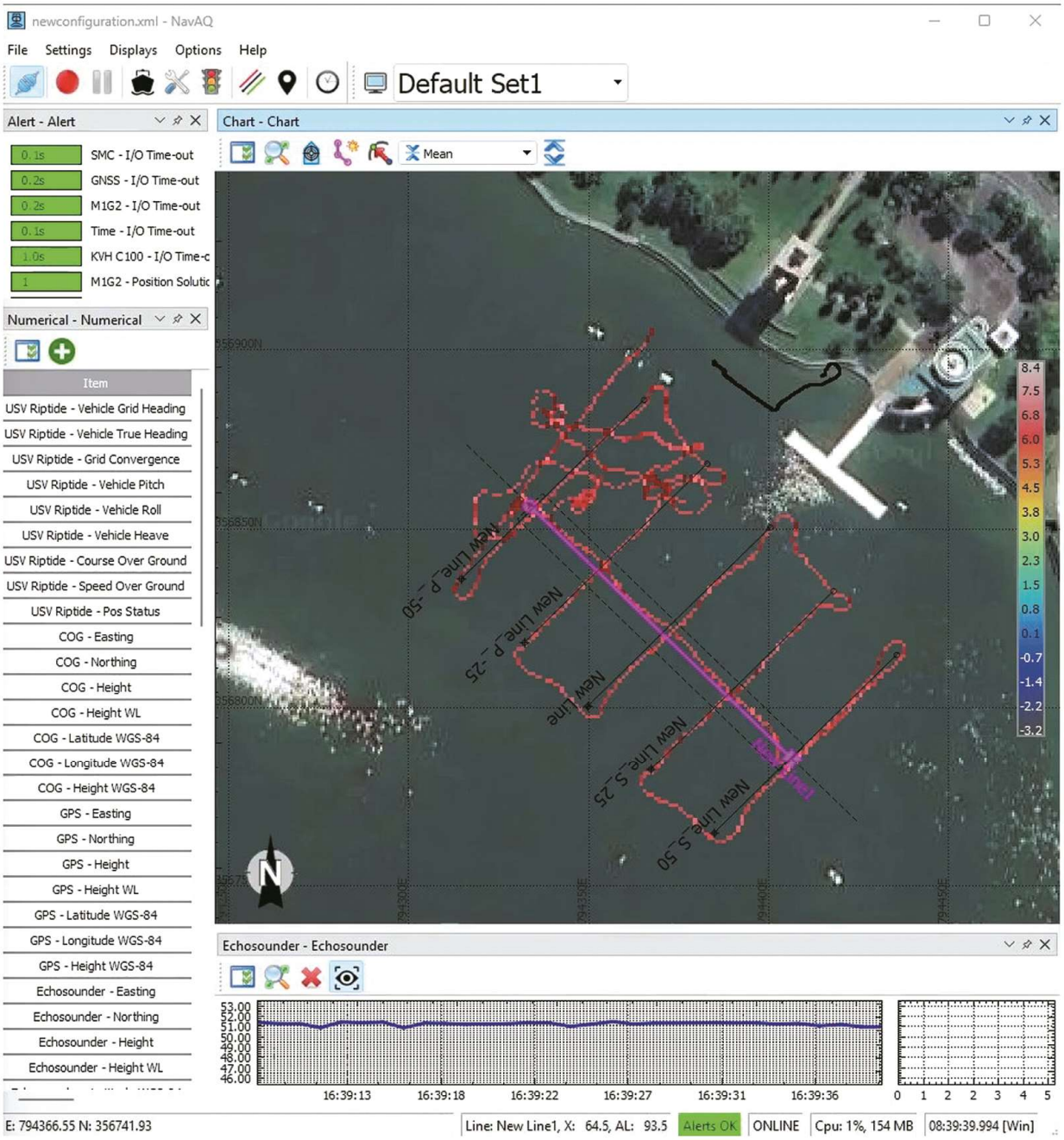

Fig. 8 — Nav Aq software interface for bathymetry data recording in the National Marine Electronics Association (NMEA) standard

Line-following navigation

Figure 9 illustrates the performance of a modernised USV during a line-following navigation task, showing the actual trajectory in red juxtaposed against the planned waypoints in blue. This visualisation not only emphasises the USV's adherence to the set course but also highlights deviations where the red path strays from the blue markers, crucial for assessing navigation system accuracy and identifying navigational challenges. A colour gradient ranging from blue to yellow is also employed to quantitatively depict the distance between the actual path and the waypoints, offering an instant visual evaluation of navigational precision. Cooler colours represent areas of minimal deviation, indicating high accuracy, while warmer colours signal significant deviations, pointing to potential areas for improvement. Such deviations could stem from

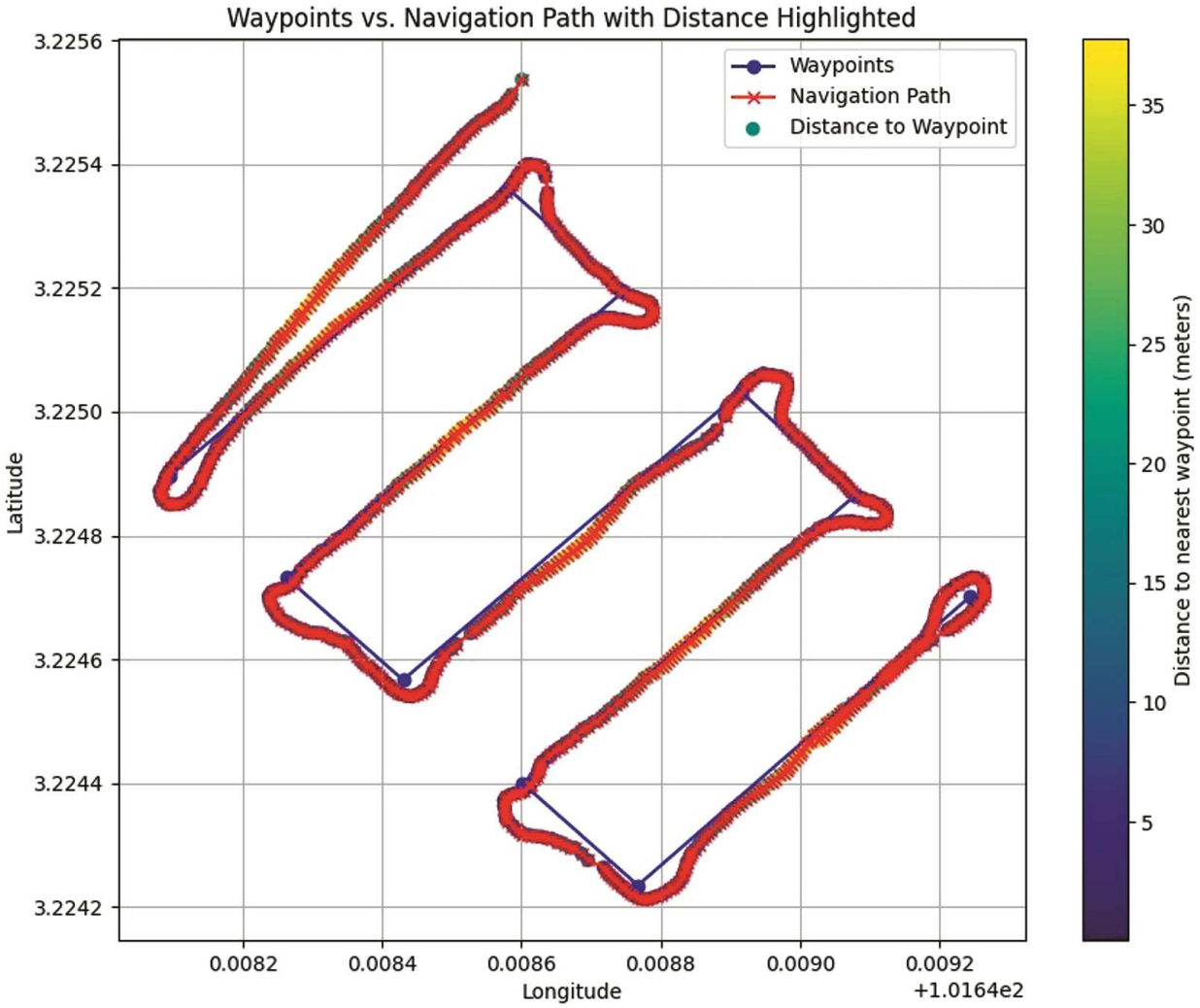

Fig. 9 — Navigational analysis of the USV in a line-following task, showing the actual versus planned paths with longitude and latitude axes, and a deviation plot highlighting navigation precision

factors including system latency, environmental influences, or limitations in dynamic positioning capabilities. Notably pronounced deviations suggest critical areas for enhancing the USV's navigation system, while sections closely aligned with the waypoints demonstrate the effectiveness of the PID control algorithms in maintaining the course in a dynamic aquatic environment.

The results encapsulate not only the efficacy of the USV's navigation system but also underline the importance of real-time data processing and adaptive control mechanisms. Results further provide insights into how different sections of the route—possibly with varying environmental conditions—affect the USV's performance. Detailed examination of these deviations, particularly in correspondence with environmental data logs, could yield improvements in predictive control algorithms, ensuring the USV maintains a tighter trajectory alignment with the waypoints.

Figure 10 extends this analysis by illustrating the cross-track error over time, highlighting how navigational accuracy fluctuates throughout the mission. Peaks in the graph indicate where the USV strayed further from its intended route, possibly due to complex manoeuvres or challenging environmental conditions. Analysing these fluctuations helps identify systematic errors and external disturbances that influence navigation, such as waves or currents. The data also provide an empirical foundation for adjusting PID control parameters to minimise such errors, thereby refining the vessel's autonomous navigation capabilities.

The graph of the USV's cross-track error reveals significant fluctuations, with peaks indicating moments where the vessel deviated notably from its intended route. These variations suggest that certain route segments may have presented more challenging conditions or required intricate manoeuvring, contributing to increased navigational errors. The periodic nature of the error might be due to repetitive environmental patterns, inherent systematic errors in the navigation system, or cyclical external disturbances like waves or currents. Additionally, the peaks in the graph likely correspond to specific waypoints or manoeuvres that posed particular challenges for the USV's navigation system, such as tight turns or areas with conflicting currents, which could lead to larger deviations from the planned path. In contrast, the troughs or lower values on the graph likely represent straighter segments or conditions where the USV could maintain a trajectory closer to the desired path. Notably, the USV demonstrates low cross-track error during straight-line navigation, which is advantageous for collecting consistent bathymetry data along the survey line, indicating commendable performance under less complex navigational conditions.

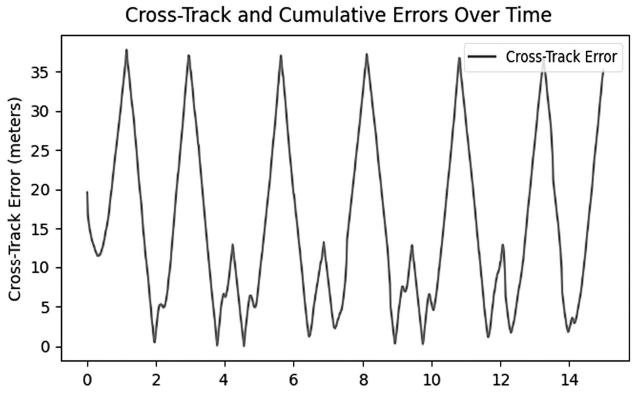

Fig. 10 — Navigation error in line-following navigation of the USV

USV map-based bathymetry survey results

Figure 11 presents a top-down view of the bathymetric data collected by the USV at Tasik Metropolitan, depicting the depth distribution across a

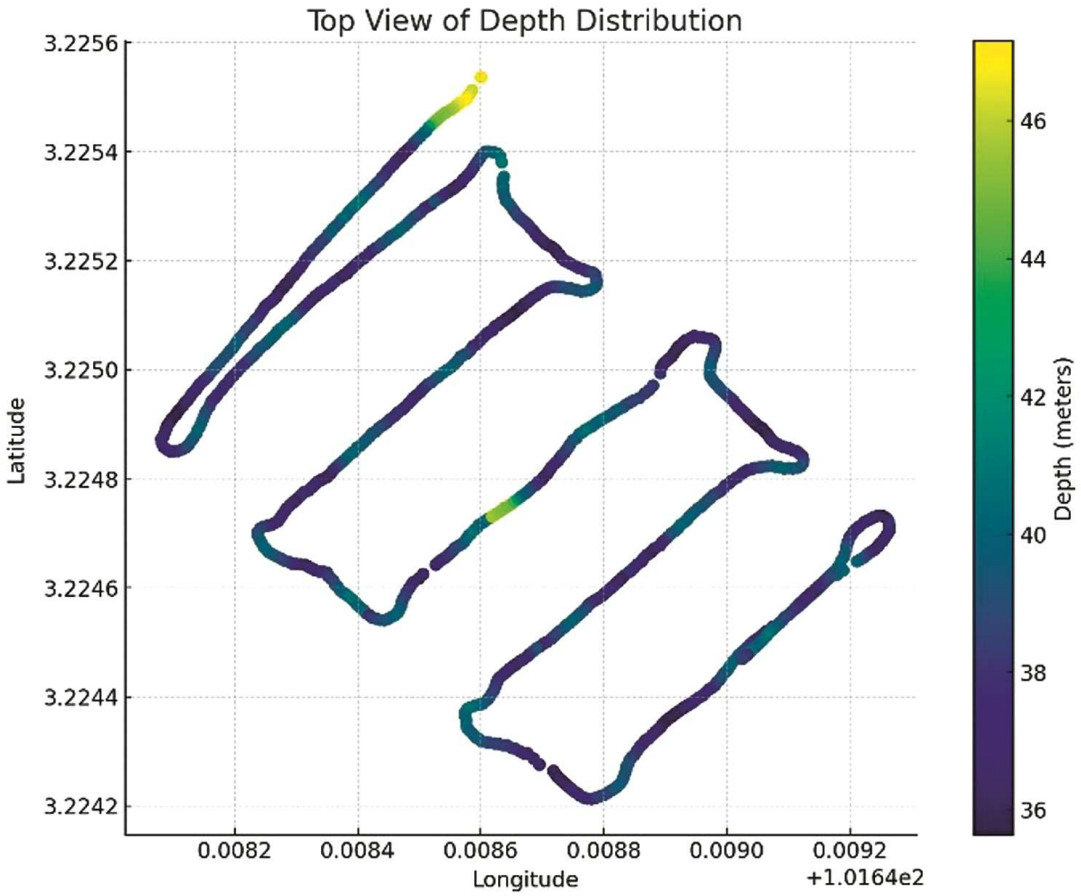

Fig. 11 — 2D plot of depth distribution from the from USV line-following navigation

water body. The data is visualised through a colour gradient on the map, with darker blues representing shallower areas and yellows indicating deeper regions. The USV's navigational path over the water is marked by coordinates, providing a geographical context to the depth measurements.

Figure 12 show cases two advanced visualisations of underwater terrain, starting with a 3D scatter plot that uses latitude and longitude for the horizontal axes and an inverted z-axis for depth, providing a bird's-eye view of the lakebed. This 3D representation is invaluable for hydrographic surveying, enhancing data utility for environmental assessments, navigational safety, and scientific research. Additionally, an interpolated 3D map of the lake bed, created through radial basis function interpolation, smoothly approximates depth values across the surveyed area. The colour scale transitions from dark blue to yellow to illustrate depth changes reveal contours and features of the lake bed where peaks indicate deeper sections and valleys suggest shallower regions.

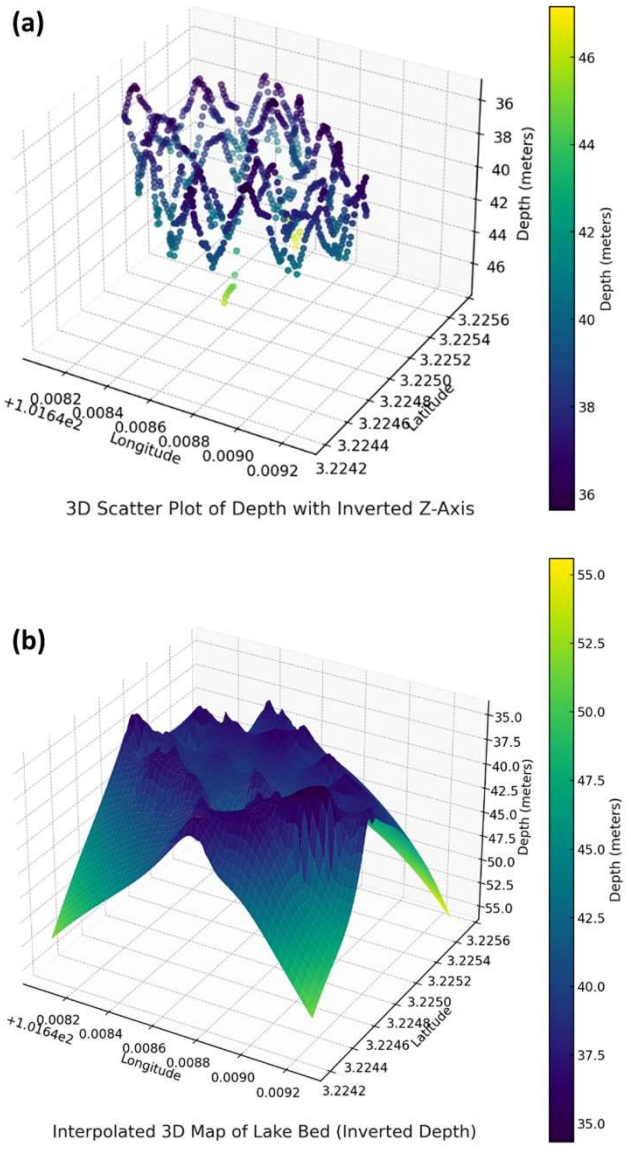

Fig. 12 — Detailed visualisation of lake bed variations: (a) 3D scatter plot showing depth variations across latitude and longitude; and (b) Interpolated 3D map of the lake bed using radial basis function interpolation

The depth readings ranging from approximately 36 to 46 m reveal a significant variance, which is crucial for understanding the bathymetric dynamics of the area. The shallowest areas, highlighted in darker blue, are critical for identifying potential navigational hazards or ecological zones of interest, possibly serving as habitats for aquatic species. Conversely, the deepest parts, shown in yellow, may represent underwater channels or depressions.

These detailed bathymetric models are pivotal for a range of applications, from ecological studies and sedimentation analysis to resource management. They also play a critical role in ensuring navigation safety and supporting engineering projects, especially in areas susceptible to flooding or where underwater structures are planned[6].

The ability to analyse these features in three dimensions not only enriches the understanding of underwater topography but also supports strategic decision-making for maritime operations and environmental conservation. Ultimately, the success of this autonomous survey operation is highlighted by the USV's ability to collect and render clear, detailed 3D visualisations of the surveyed depths, showcasing the advanced capabilities of modern hydrographic surveying techniques[5].

Discussion

The outcomes of this study confirm the USV's capability to navigate and accurately collect depth data, achieving a CTE of just 0.92 to 2.39 m, which significantly surpasses the International Hydrographic Organization's Category 2 standards. However, the trajectory plot indicates instances where CTE exceeded 35 m, suggesting the need for further investigation into these discrepancies. These deviations can be attributed to external disturbances such as wind, currents, and waves, which affect the USV's stability and accuracy. Additionally, system latencies and sensor inaccuracies, including GNSS errors and IMU drift, contribute to these variations. Enhanced sensor fusion and adaptive control

algorithms can mitigate these issues by improving the robustness of positional estimates and responsiveness to environmental conditions.

Despite the overall high precision, the observed deviations in the vessel's trajectory in areas with complex underwater structures or dynamic environmental conditions highlight opportunities for algorithmic improvement. Specifically, the systematic errors identified by peaks in cross-track error, averaging 1.5 m in more complex regions, suggest that enhancements in the USV's sensor fusion algorithms or adjustments in the PID control parameters could refine its adaptability to environmental variabilities. Suboptimal tuning of PID controllers, such as aggressive tuning causing oscillations or conservative tuning leading to sluggish responses can be addressed by iterative testing and optimisation. The IMO standards refer to manoeuvring parameters and track errors regarding the unit vessel's Overall Length (OAL). Considering this, findings of the current study indicate that the USV's performance aligns well with these standards, maintaining track errors within acceptable limits relative to its OAL.

The variations in cross-track errors during straight-line navigation are influenced by several factors. Environmental disturbances such as wind, currents, and waves significantly impact the USV's ability to maintain its intended course. Sudden gusts or sustained winds can push the vessel off track while varying currents in shallow waters exert lateral forces that affect its stability. Wave action causes the USV to pitch and roll, leading to temporary deviations. System latencies in sensor data acquisition and actuator response introduce delays in navigation corrections, resulting in increased CTE. Sensor inaccuracies, including GNSS errors due to multipath effects or signal obstructions and IMU drift, also contribute to inaccurate positional data and errors in heading and attitude estimation. Addressing these factors through enhanced sensor fusion, adaptive control algorithms, regular sensor calibration, and incorporating real-time environmental data into the navigation algorithm can significantly reduce navigation errors.

Looking ahead, the vessel's Guidance, Navigation, and Control (GNC) system is set for substantial advancements. Future developments will likely focus on refining the autonomy of the GNC algorithms and enhancing the synergy between the multi-GNSS system and inertial navigation. The potential incorporation of machine learning techniques could reduce manual interventions by predicting and adjusting for navigational anomalies, improving path adherence with an anticipated 30 % increase in navigation precision. Moreover, ongoing developments in dual-frequency GNSS receivers and the application of advanced measurement techniques promise to augment the USV's positioning accuracy, potentially reducing average positional errors to below 0.5 m, thus pushing the boundaries of what is achievable in autonomous hydrographic surveying.

Conclusion

This study demonstrates significant advancements in hydrographic surveying, showcasing the precision of the USV equipped with modern technology like the CXSense controller, M1G2 GNSS, KVH C100 magnetic compass, and SBG System INS. The USV maintained course accuracy within CTE of 0.92 to 2.39 m, exceeding the International Hydrographic Organization's Category 2 standards. Comprehensive upgrades to the USV's propulsion, positioning, control, and data transmission systems facilitated automated operations and enhanced performance in ultra-shallow waters. The successful use of cost-effective multi-GNSS receivers indicates a shift towards more economical yet efficient hydrographic survey methodologies, suggesting that these technologies could replace expensive professional equipment without compromising quality, potentially revolutionising maritime applications by improving the accessibility and sustainability of hydrographic data collection.

Acknowledgements

The author gratefully acknowledges the support from the IIUM Engineering Merit Scholarship (KOEIEMS) for outstanding students. This scholarship has significantly contributed to the completion of research presented in this paper. This work was supported in part by the Ministry of Higher Education (MoHE) Malaysia and International Islamic University Malaysia (IIUM); in part by the Research Management Centre; in part by the project MyLAB22-002-0002CXSense System for the SURAYA Unmanned Surface Vessel Fleet; and in part by Hidrokinetik Technologies Sdn Bhd as the industrial partner.

Conflict of Interest

The authors state that there are no conflicts of interest with any organisations or funding bodies.

Funding

This work was supported in part by the Ministry of Higher Education (MoHE) Malaysia through a collaborative effort between Hidrokinetik Technologies Sdn Bhd and International Islamic University Malaysia (IIUM); in part by the Research Management Centre; and in part by the project MyLAB22-002-0002 CXSense System for the SURAYA Unmanned Surface Vessel Fleet.

Ethical Statement

All authors agreed to the ethical principles.

Author Contributions

MAN & TATA: Conceptualization, investigation, methodology, and writing original draft. ZZA: Supervision & validation, reviewing & editing and funding acquisition.

Nomenclature

x	Position along the x-axis (longitudinal axis)	T	Current thruster force of USV
y	Position along the y-axis (lateral axis)	S_{rudder}	Rudder sensitivity of USV
z	Vertical position in the global coordinate	$S_{thurster}$	Thrust sensitivity of USV
V	Current speed of USV	V_d	Desired speed of the USV
θ	Current heading of USV	θ_d	Desired heading of the USV
ϕ	Current angle of USV rudder	ϕ_d	Desired angle of USV rudder
T_d	Desired thrust exerted by the propulsion system	$\frac{d}{dt}e_\theta$	Derivative of heading error
Kp_θ	Proportional gain for heading	PID_θ	PID controller output for heading
Ki_θ	Integral gain for heading	PID_V	PID controller output for speed
Kd_θ	Derivative gain for heading	$e_{\theta,prev}$	Previous heading error
Kp_V	Proportional gain for speed	$e_{V,prev}$	Previous speed error
Ki_V	Integral gain for speed	$\Delta\theta_{tol}$	Heading tolerance
Kd_V	Derivative gain for speed	ΔV_{tol}	Speed tolerance
$\int e_\theta$	Heading error Integral of USV		

Greek Symbols

ψ	Heading angle	θ	Pitch angle
φ	Roll angle		

Abbreviations

USV	Unmanned Surface Vessel	BLDC	Brushless DC Motors
GNSS	Global Navigation Satellite Systems	ESCs	Electronic Speed Controllers
DGPS	Differential Global Positioning System	LiPo	Lithium Polymer
INS	Inertial Navigation System	IHO	International Hydrographic Organization
SBES	Single Beam Echo Sounder	UDP	User Datagram Protocol
MBES	Multi Beam Echo Sounder	GNC	Guidance, Navigation, and Control

References

1 Specht M, Stateczny A, Specht C, Widźgowski S, Lewicka O, *et al.*, Concept of an innovative autonomous unmanned system for bathymetric monitoring of shallow waterbodies (INNOBAT System), *Energies*, 14 (17) (2021) p. 5370. https://doi.org/10.3390/en14175370

2 Gourcuff C, Lherminier P, Mercier H & Le Traon P Y, Altimetry combined with hydrography for ocean transport estimation, *J Atmos Ocean Technol*, 28 (10) (2011) 1324–1337. https://doi.org/10.1175/2011JTECHO818.1

3 Weatherall P, Marks K M, Jakobsson M, Schmitt T, Tani S, *et al.*, A new digital bathymetric model of the world's oceans, *Earth Space Sci*, 2 (8) (2015) 331–345. https://doi.org/10.1002/2015EA000107

4 Jakobsson M, Mayer L, Coakley B, Dowdeswell J A, Forbes S, *et al.*, The International Bathymetric Chart of the Arctic Ocean (IBCAO) Version 3.0, *Geophys Res Lett*, 39 (12) (2012) p. L12609. https://doi.org/10.1029/2012GL052219

5 Liu Y, Wu Z, Zhao D, Zhou J, Shang J, *et al.*, Construction of High-Resolution Bathymetric Dataset for the Mariana Trench, *IEEE Access*, 7 (2019) 142441–142450. https://doi.org/10.1109/ACCESS.2019.2944667

6 Lubczonek J, Kazimierski W, Zaniewicz G & Lacka M, Methodology for Combining Data Acquired by Unmanned Surface and Aerial Vehicles to Create Digital Bathymetric Models in Shallow and Ultra-Shallow Waters, *Remote Sens*, 14 (1) (2021) p. 105. https://doi.org/10.3390/rs14010105

7 Marchel Ł, Specht C & Specht M, Assessment of the Steering Precision of a Hydrographic USV along Sounding Profiles Using a High-Precision GNSS RTK Receiver Supported Autopilot, *Energies*, 13 (21) (2020) p. 5637. https://doi.org/10.3390/en13215637

8 Zhao L & Bai Y, Unlocking the Ocean 6G: A Review of Path-Planning Techniques for Maritime Data Harvesting Assisted by Autonomous Marine Vehicles, *J Mar Sci Eng*, 12 (1) (2024) p. 126. https://doi.org/10.3390/jmse12010126